

# Investigation of Quantum Dot Color Filter Micro-LED Display

Xuhui PENG<sup>1,2,3</sup>, Yang ZENG<sup>3</sup>, Sitao HUO<sup>3</sup>, Zhenyuan YANG<sup>1</sup>,  
Xiaoping HUANG<sup>1,2\*</sup>, and Qing ZHAO<sup>1,2\*</sup>

<sup>1</sup>*School of Resources and Environment, University of Electronic Science and Technology of China, Chengdu 611731, China*

<sup>2</sup>*Yangtze Delta Region Institute (Huzhou), University of Electronic Science and Technology of China, Huzhou 313001, China*

<sup>3</sup>*Shanghai Tianma Microelectronics, Shanghai 201201, China*

\*Corresponding authors: Xiaoping HUANG and Qing ZHAO  
E-mail: xphuang@uestc.edu.cn and zhaqq@uestc.edu.cn

**Abstract:** In this work, we present the investigation of the quantum dot color filter (QDCF) micro-light emitting diode (micro-LED) display. Green and red quantum dot photoresist (QDPR) materials are patterned into a pixelated array and precisely bonded with an all-blue micro-light emitting diode (micro-LED) substrate, forming a red, green, and blue (RGB) full color display through color conversion. A few factors that influence the achievable color gamut are further investigated. The resulting 1.1-inch 228-pixels per inch (ppi) display demo shows the good performance. The findings in this paper pave a way to the future industrialization of the micro-LED display.

**Keywords:** Quantum dot color filter (QDCF), color conversion, micro-light emitting diode (micro-LED), color gamut

---

Citation: Xuhui PENG, Yang ZENG, Sitao HUO, Zhenyuan YANG, Xiaoping HUANG, and Qing ZHAO, "Investigation of Quantum Dot Color Filter Micro-LED Display," *Photonic Sensors*, 2024, 14(1): 240123.

---

## 1. Introduction

The micro-light emitting diode (micro-LED) display has been one of the main research focuses in the display industry in recent years [1–10]. It is a self-emitting display that possesses a high contrast ratio, like the organic light-emitting diode (OLED) [11–14], while being more robust and reliable than OLED due to its inorganic nature [1, 4, 12]. The potential for reaching ultra-high pixels per inch (ppi) also makes the micro-LED display ideal for augmented reality and virtual reality (AR/VR) applications. Thus, it has been widely considered as the next generation of the display technology and beyond [1, 4, 15–20]. However, its industrialization

has met many difficulties. One of the key challenges is the mass transfer process. The individual micro-LEDs must be transferred onto the display backplane in a massive number, which is costly and time consuming. This is even worsened by the fact that red, green, and blue (RGB) micro-LEDs come from different substrates and need to be transferred separately, tripling the difficulty [8, 9, 12]. Another main challenge is the different temperature dependence of the emission efficiency of RGB micro-LEDs. At a high temperature, the efficiency of red micro-LED usually drops much faster than that of blue or green LEDs, leading to a notable color shift.

Received: 5 June 2023 / Revised: 29 August 2023

© The Author(s) 2023. This article is published with open access at Springerlink.com

DOI: 10.1007/s13320-023-0698-5

Article type: Regular

In light of these challenges, the quantum dot color filter (QDCF) has been proposed as an alternative method to realize the full color micro-LED display [2, 13, 17]. In this technology, the quantum dot (QD) containing material, such as the quantum dot photoresist (QDPR) or quantum dot ink, is patterned into a pixelated array by photolithography or ink jet printing. Then this QDCF top glass is mounted on an all-blue micro-LED backplane with pixel-to-pixel precision. Red QDs (R-QDs) and green QDs (G-QDs) in the red and green sub-pixels would then convert the emitted blue light from blue micro-LEDs into red and green light, respectively, realizing a full color display. In this way, only a monochrome blue micro-LED backplane is needed, which greatly simplifies the mass transfer process and also alleviates the temperature induced color shift.

In this paper, we present our investigation of the QDCF micro-LED technology. We use photolithography to pattern red and green QDPRs on the QDCF top glass. Then, this top glass is precisely bonded with a blue micro-LED backplane. Optical performance of the resulted device is measured. Furthermore, we discuss the influence of the blue light emission angle on the proper choice of the QDPR thickness and the optimization of the precision bonding process to eliminate the crosstalk. As a result, we have achieved a 1.11-inch 228-ppi full color QDCF micro-LED prototype with the good display performance. The discussion may facilitate the application of the QDCF technology in micro-LED displays.

## 2. Experimental method

### 2.1 Fabrication of QDCF top glass

Figure 1 shows the schematic drawing of a QDCF micro-LED. The device consists of the QDCF top glass and a blue micro-LED backplane. The QDCF top glass further consists of many parts. The R-QDs and G-QDs layers perform the color

conversion process. A color free photoresist (CFPR) is added in the blue sub-pixel which contains TiO<sub>2</sub> nano-particles that scatter blue light into a Lambertian distribution. This ensures that the blue light angular distribution matches that of the QD emission, eliminating the color shift at the increased viewing angle. A separation bank is formed between sub-pixels, which is also a patterned opaque photoresist layer. The bank has several functions, and the most important one is to block light leakage from neighboring sub-pixels and ensure the good color gamut. Other functions include assisting the definition of the QDPR/CFPR pattern, and supporting the cell structure when the top glass is bonded with the backplane. Apart from the above layers, the QDCF top glass further consists of a conventional color filter (CF) structure, including a black matrix (BM) and red, green, and blue (RGB) CFs. The main purpose of this conventional CF structure is to absorb the non-converted blue emission from red and green sub-pixels to ensure color purity, while also functioning as an anti-reflection layer to ensure a black appearance of the device.

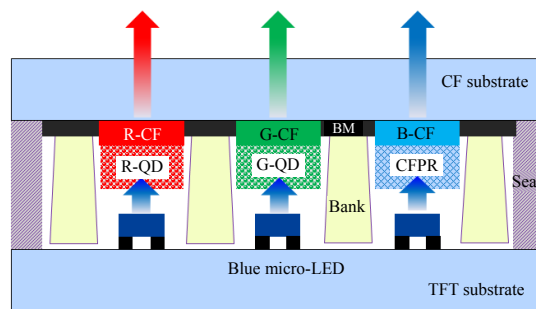


Fig. 1 Schematic drawing of a QDCF micro-LED, wherein the thin film transistor (TFT) substrate is the micro-LED backplane.

To achieve the above-described target structure, the QDCF top glass is fabricated by a process flow shown in Fig. 2(a). First is the formation of a conventional CF structure by photolithography of respective materials, which is well known to the liquid crystal display (LCD) industry so is not shown here in detail. A silicon nitride and silicon oxide double-layer buffer is then deposited by the

plasma enhanced chemical vapor deposition (PECVD) onto the CF to provide good adhesion force for the subsequent bank material. A first bank layer is formed by spin coating the bank material followed by photolithography into the desired pattern with openings matching the micro-LED pixels. The thickness of the first bank is limited to 8  $\mu\text{m}$  due to the difficulty in exposure through a thicker layer of the bank material. Then, the CFPR, R-QD, and G-QD are sequentially formed into the bank opening by spin coating and photolithography. These materials are bought from Sumitomo Chemical Co., Ltd., Japan and the QDs are the InP-based Cd-free type. Here, the CFPR is formed first to reduce the degradation of the QD from the subsequent ultraviolet (UV) exposure and annealing. Finally, a second bank of 8- $\mu\text{m}$  thickness is formed by a similar process to achieve sufficient total bank height for the crosstalk elimination and mechanical support. A scanning electronic microscopy (SEM) image of the completed QDCF top glass is shown in Fig. 2(b).

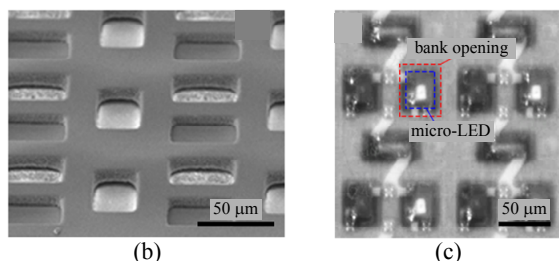
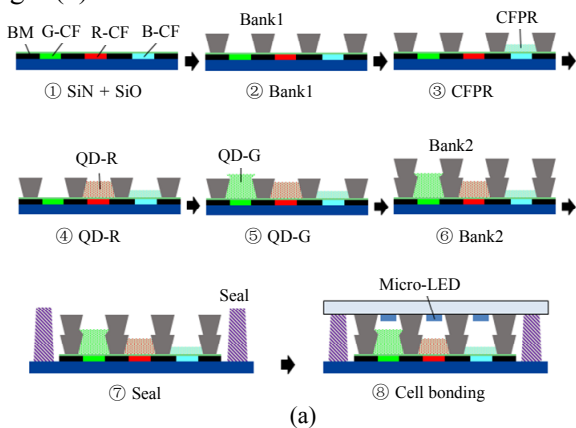


Fig. 2 Process flow of the QDCF micro-LED: (a) fabrication process of the QDCF micro-LED device, (b) SEM image of QDCF top glass, and (c) optical microscope (OM) image of the precision-alignment process.

## 2.2 Bonding of QDCF with micro-LED substrate

The QDCF top glass is first cut into the 1.1-inch single panel size. The blue micro-LED backplane is formed by mass transferring blue micro-LED chips onto a low temperature poly-crystalline (LTPS) TFT backplane and then cut into the 1.1-inch single panel size. Precision bonding of the QDCF top glass and micro-LED backplane is the key process in fabricating a QDCF micro-LED. The bonding precision in the  $x$ - $y$  plane needs to be within about  $\pm 5 \mu\text{m}$  to avoid the collision between the bank and micro-LED chip. Otherwise, the chip may be damaged or cannot fit into the bank opening and produces significant crosstalk. Meanwhile, the tight contact between the QDCF top glass and micro-LED backplane in the  $z$  direction is also critical. A uniform tight contact across the display area is needed to ensure the homogenous pure color. This will be further discussed in Section 3.

The precision bonding is carried out on the Finetech fine placer equipment. Alignment marks are made on the top glass and backplane, respectively, during their photolithography processes. Before bonding, the sealant material is coated on the periphery of the top glass and pre-cured by UV. Then the top glass and backplane are aligned pixel-to-pixel and pressed together. In this step, fine tuning of the position can be carried out with the help of in-situ OM monitoring, which is shown in Fig. 2(c). Finally, the complete QDCF micro-LED module is heated to cure the sealant and fix the position of the top glass and backplane.

## 3. Results and discussion

We have fabricated several iterations of the 1.1-inch QDCF micro-LED device, with the aim of improving the color gamut and uniformity. Many design and process aspects must be considered carefully to achieve the good optical performance. Here we discuss two of them that significantly influence the final color gamut. The first item is the influence of the blue emission angular distribution on the converted color purity. In a QD color

conversion device, the thickness of the QD layer is a key factor. If the QD layer thickness is too thin, it cannot effectively absorb the blue source light. This not only limits the conversion efficiency, but also affects the color purity, since the CF cannot cut off all blue leakage completely. On the other hand, if the QD layer is too thick, it also lowers the conversion efficiency due to the self-absorption of the converted red/green emission. Thus, the ideal QD layer thickness must be found.

In our initial attempts of the fabrication, we have first measured the converted spectra of R-QDs and G-QDs with the varying thickness under the illumination of a blue micro-LED panel. The color coordinates of the converted red and green light are measured, and the color gamut is calculated. It is found that for green light, an 8  $\mu\text{m}$ -thick QD layer is sufficient to achieve 90% of the National Television Standards Committee (NTSC) color gamut, assuming zero crosstalk. However, when we fabricate a QDCF micro-LED with an 8  $\mu\text{m}$ -thick G-QD layer, the final G frame looks cyan, as shown by the OM image in Fig. 3(a). It can be seen that the converted color in an actual QDCF micro-LED device is very different from the one that predicts from a uniform QD layer placed on the same blue micro-LED panel light source, as shown in the photo of Fig. 3(b). The spectrum comparison of the module and film is shown in Fig. 3(c). We can see that the blue leakage in the module is much more severe than that of the film. Note that the shift in the peak wavelength of the blue leakage is due to the filtering effect of the G-CF, which is presented in both cases. Such discrepancy is found to be caused by the difference of the blue light angular distribution. In the case of a QD film on the top of a planar blue light source, the light source is quasi-Lambertian and illuminates the QD layer with a wide angle. These oblique incident rays travel a longer distance within the QD layer, increasing their effective optical paths and the chances of conversion. However, in a QDCF micro-LED device, the blue micro-LED illuminates the QD layer mostly from

beneath rather than from a large oblique angle. Thus, the average optical path in the QD is much shorter than that in the case of the planar light source, lowering its conversion capability.

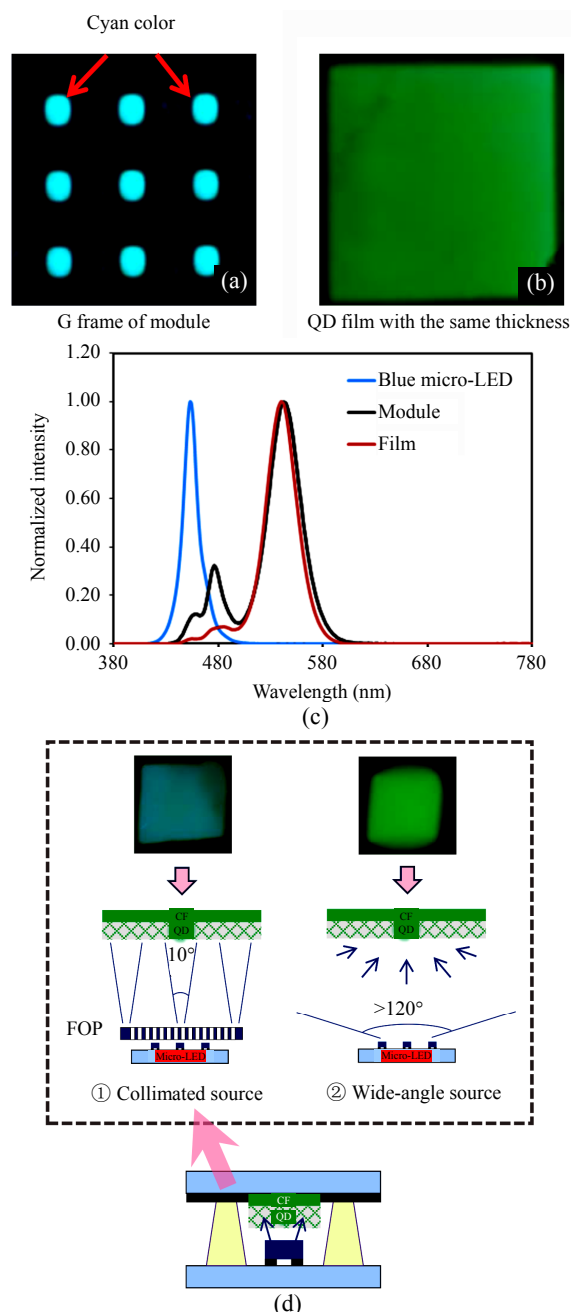


Fig. 3 Cyan color issue of QDCF micro-LED: (a) cyan color of G frame in the initial fabrication, (b) G-QD film with the same thickness placed above the same blue micro-LED light source, (c) spectra comparison between the module and film, and (d) influence of the blue emission angular distribution on the converted color purity. FOP: fiber optical plate.

We have verified this effect experimentally as shown in Fig. 3(d). We add an FOP between the

planar blue micro-LED light source and the QD film, which limits the transmitted blue light to a cone of about  $10^\circ$ . In this case, the QD film appears cyan, indicating a notable amount of un-absorbed blue light. By contrast, without this FOP, the same QD film has a desired green appearance. The contrast well proves the dependence of the converted color purity on the angular distribution of the light source. With this in mind, we have re-calibrated the dependence of the converted spectrum on the QD thickness by testing QD films of different thickness under collimated illumination. The result is shown in Fig. 4.

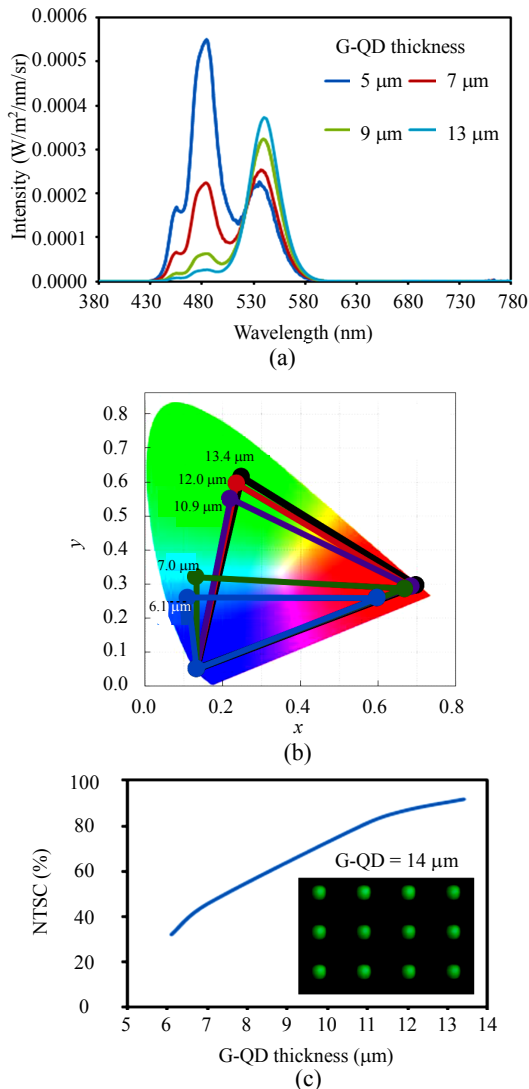


Fig. 4 Calibration of target G-QD thickness: (a) measured spectra of G-QD film under a  $10^\circ$  incidence blue light source, (b) corresponding color gamut, and (c) calculated NTSC. Insert: OM image of the fabricated module with  $14 \mu\text{m}$ -thick G-QD.

Figure 4(a) shows the measured spectra of the G-QD film under a  $10^\circ$  incidence blue light source, while Figs. 4 (b) and 4(c) show the calculated color gamut and NTSC based on the spectra. The G-QD thickness of  $13.4 \mu\text{m}$  instead of  $8 \mu\text{m}$  is needed to achieve  $>90\%$  NTSC. Finally, in later iterations of the fabrication, we have chosen the G-QD thickness of  $14 \mu\text{m}$ , and the resulting G frame exhibits a pure green color, as shown by the OM image in the insert of Fig. 4(c).

The second item that can significantly impact the final color gamut is the crosstalk between neighboring pixels. Many factors can contribute to this issue, including the blue light transmission through the bank and reflection from the array layers. In our work, we find that the key limiting factor is the evenness of the substrates in the precision bonding process, in other words, the suppression of center bulging of the CF top glass. In Fig. 5(a), the color diagram shows the measured color gamut in some of our initial samples. The periphery of the sample shows the good color gamut of up to  $82\%$  NTSC, while the center part is much worse, achieving only  $55.2\%$  NTSC. Comparing the color coordinates, we can easily see that the shrinking color gamut is due to the shift of green and red color coordinates towards the blue one, implying the blue light leakage. The appearance of the sample displaying a red frame is shown below by the left photo of Fig. 5(b). The center part appears purple, and under OM we can see blue light leakage through the adjacent blue sub-pixel. To identify the cause of issue, we measure the thickness of the sample by a micrometer. The center part is about  $2 \mu\text{m}$ – $3 \mu\text{m}$  thicker than the periphery, indicating the existence of bulging. In this case, the bank in the center part does not uniformly touch the array substrate, allowing blue light to directly leak to neighboring pixels and contribute to the wrong color. This mechanism is illustrated by Fig. 5(c), and is further proved by the spectrum comparison in Fig. 5(d), where the center part has much higher blue leakage compared with the periphery.



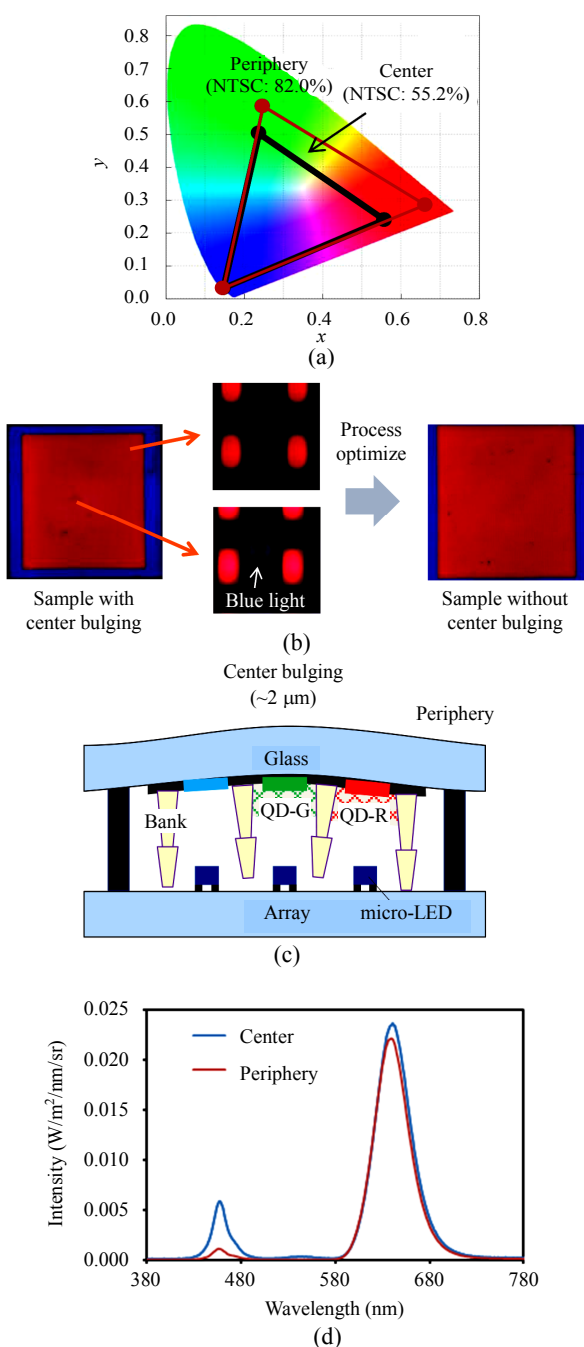


Fig. 5 Center bulging issue of QDCF micro-LED: (a) color gamut comparison between the center and periphery, (b) eliminating crosstalk induced by the center bulging during precision bonding process, (c) illustration of the center bulging phenomenon, and (d) spectra comparison between the center and periphery.

To solve this issue, we have optimized many aspects of the design and process. Firstly, the precision bonding equipment is re-adjusted before the bonding. The evenness of the stage is calibrated multiple times by using the pressure-sensitive paper

before bonding the sample. Secondly, air jet cleaning is used to remove particles from both substrates to ensure the tightness of the bonding. Thirdly, we have optimized the pre-curing process of the seal. The seal is first pre-cured with UV before lamination and then cured by heating. We find that the modulus of the seal after pre-curing increase very rapidly after about 15 min. So if the bonding takes place too long after pre-curing, the seal is too stiff to be deformed and will bounce back when the bonding pressure is removed. In this case, center bulging may appear. Finally, we have optimized the design of the supporting bank pattern in the periphery of the panel, allowing for better mechanical support and thus overall evenness. With all these countermeasures being in place, we have achieved very good color gamut uniformity across the whole display area, as shown in the rightmost photo in Fig. 5(b).

Finally, Fig. 6 shows the photo and specifications of our 1.1-inch 228-ppi QDCF



Item	Specification
Size	1.1 inch
Resolution	180 × 180 pixels
ppi	228
Pixel pitch	111 μm



Fig. 6 Photos of the 1.1-inch 228-ppi QDCF micro-LED prototype, its specification, and display images.

prototype. The resolution is  $180 \times 180$  pixels and the pixel pitch is  $111 \mu\text{m}$ . The prototype specification is suitable for smart watches but the design principles can be extended to a wide variety of other applications. Some images displayed by the prototype are shown in the bottom of Fig. 6, demonstrating the good uniformity and vivid color.

#### 4. Conclusions

In summary, we have investigated the fabrication of the QDCF micro-LED display. The QDCF top glass is fabricated by photolithography of the respective photoresist material, and the top glass is then precisely bonded with a blue micro-LED backplane to achieve a full color micro-LED display. Two key factors, which significantly affect the color gamut, have been discussed, and the countermeasures are provided. With the design and process optimization, the resulting 1.1-inch 228-ppi QDCF micro-LED prototype shows the good display performance. As the QDCF micro-LED is gaining increasing attention in the display industry, understanding and eliminating the color crosstalk will be of vital importance. The selection of the correct QD film thickness and optimization of the precision bonding process discussed in this work will provide a useful guideline in this area. The findings in this work prove the potential for the color conversion technology in the commercialization of the micro-LED and may pave the way to the further research.

#### Acknowledgment

This work was supported by Sichuan Science and Technology Program (Grant No. 2023YFH0089).

#### Declarations

**Conflict of Interest** The authors declare that they have no competing interests.

**Open Access** This article is distributed under the terms of the Creative Commons Attribution 4.0 International License (<http://creativecommons.org/licenses/by/4.0/>), which permits unrestricted use,

distribution, and reproduction in any medium, provided you give appropriate credit to the original author(s) and the source, provide a link to the Creative Commons license, and indicate if changes were made.

#### References

- [1] Y. Huang, E. L. Hsiang, M. Y. Deng, and S. T. Wu, "Mini-LED, micro-LED and OLED displays: present status and future perspectives," *Light: Science & Applications*, 2020, 9(1): 105 (2020).
- [2] Y. M. Huang, J. H. Chen, Y. H. Liou, K. James Singh, W. C. Tsai, J. Han, *et al.*, "High-uniform and high-efficient color conversion nanoporous GaN-based micro-LED display with embedded quantum dots," *Nanomaterials*, 2021, 11(10): 2696.
- [3] S. S. Pasayat, C. Gupta, M. S. Wong, R. Ley, M. J. Gordon, S. P. DenBaars, *et al.*, "Demonstration of ultra-small ( $< 10 \mu\text{m}$ ) 632 nm red InGaN micro-LEDs with useful on-wafer external quantum efficiency ( $> 0.2\%$ ) for mini-displays," *Applied Physics Express*, 2020, 14(1): 011004.
- [4] T. Wu, C. W. Sher, Y. Lin, C. F. Lee, S. Liang, Y. Lu, *et al.*, "Mini-LED and micro-LED: promising candidates for the next generation display technology," *Applied Sciences*, 2018, 8(9): 1557.
- [5] H. V. Han, H. Y. Lin, C. C. Lin, W. C. Chong, J. R. Li, K. J. Chen, *et al.*, "Resonant-enhanced full-color emission of quantum-dot-based micro LED display technology," *Optics Express*, 2015, 23(25): 32504–32515.
- [6] X. Zhou, P. Tian, C. W. Sher, J. Wu, H. Liu, R. Liu, *et al.*, "Growth, transfer printing and colour conversion techniques towards full-colour micro-LED display," *Progress in Quantum Electronics*, 2020, 71: 100263.
- [7] H. W. Choi, C. Liu, E. Gu, G. McConnell, J. M. Girkin, I. M. Watson, *et al.*, "GaN micro-light-emitting diode arrays with monolithically integrated sapphire microlenses," *Applied Physics Letters*, 2004, 84(13): 2253–2255.
- [8] A. Paranjpe, J. Montgomery, S. M. Lee, and C. Morath, "Invited paper: micro-LED displays: key manufacturing challenges and solutions," *SID Symposium Digest of Technical Papers*, 2018, 49(1): 597–600.
- [9] C. C. Lin, Y. H. Fang, M. J. Kao, P. K. Huang, F. P. Chang, L. C. Yang, *et al.*, "Ultra-fine pitch thin-film micro LED display for indoor applications," *SID Symposium Digest of Technical Papers*, 2018, 49(1): 782–785.
- [10] Y. Li, J. Tao, Y. Zhao, J. Wang, J. Lv, Y. Qin, *et al.*, "48  $\times$  48 pixelated addressable full-color micro display based on flip-chip micro LEDs," *Applied Optics*, 2019, 58(31): 8383–8389.
- [11] Z. Liu, C. H. Lin, B. R. Hyun, C. W. Sher, Z. Lv, B. Luo, *et al.*, "Micro-light-emitting diodes with

- quantum dots in display technology,” *Light: Science & Applications*, 2020, 9(1): 83 (2020).
- [12] C. A. Bower, M. A. Meitl, B. Raymond, E. Radauscher, R. Cok, S. Bonafede, *et al.*, “Emissive displays with transfer-printed assemblies of  $8\ \mu\text{m} \times 15\ \mu\text{m}$  inorganic light-emitting diodes,” *Photonics Research*, 2017, 5(2): A23–A29.
- [13] W. Bai, T. Xuan, H. Zhao, S. Shi, X. Zhang, T. Zhou, *et al.*, “Microscale perovskite quantum dot light-emitting diodes (micro-PeLEDs) for full-color displays,” *Advanced Optical Materials*, 2022, 10(12): 2200087.
- [14] L. Wang, L. Wang, C. J. Chen, K. C. Chen, Z. Hao, Y. Luo, *et al.*, “Green InGaN quantum dots breaking through efficiency and bandwidth bottlenecks of micro-LEDs,” *Laser & Photonics Reviews*, 2021, 15(5): 2000406.
- [15] R. Lin, X. Liu, G. Zhou, Z. Qian, X. Cui, and P. Tian, “InGaN micro-LED array enabled advanced underwater wireless optical communication and underwater charging,” *Advanced Optical Materials*, 2021, 9(12): 2002211.
- [16] M. S. Islim, R. X. Ferreira, X. He, E. Xie, S. Videv, S. Viola, *et al.*, “Towards 10 Gb/s orthogonal frequency division multiplexing-based visible light communication using a GaN violet micro-LED,” *Photonics Research*, 2017, 5(2): A35–A43.
- [17] H. Y. Lin, C. W. Sher, D. H. Hsieh, X. Y. Chen, H. M. P. Chen, T. M. Chen, *et al.*, “Optical cross-talk reduction in a quantum-dot-based full-color micro-light-emitting-diode display by a lithographic-fabricated photoresist mold,” *Photonics Research*, 2017, 5(5): 411–416.
- [18] S. Mei, X. Liu, W. Zhang, R. Liu, L. Zheng, R. Guo, *et al.*, “High-bandwidth white-light system combining a micro-LED with perovskite quantum dots for visible light communication,” *ACS Applied Materials & Interfaces*, 2018, 10(6): 5641–5648.
- [19] Y. Chen, B. Xie, J. Long, Y. Kuang, X. Chen, M. Hou, *et al.*, “Interfacial laser induced graphene enabling high performance liquid solid triboelectric nanogenerator,” *Advanced Materials*, 2021, 33(44): 2104290.
- [20] Z. Liu, J. Li, and X. Liu, “Novel functionalized BN nanosheets/epoxy composites with advanced thermal conductivity and mechanical properties,” *ACS Applied Materials & Interfaces*, 2020, 12(5): 6503–6515.